Chemosphere 162 (2016) 80–90

Contents lists available at ScienceDirect

Chemosphere

journal homepage: www.elsevier.com/locate/chemosphere

Pollution status of polycyclic aromatic hydrocarbons in surface sediments from the Yangtze River Estuary and its adjacent coastal zone

Chenglong Wang [a, b], Xinqing Zou [a, b, *], Jianhua Gao [a, b], Yifei Zhao [a, b], Wenwen Yu [a, b, c], Yali Li [a, b], Qiaochu Song [a, b]

[a] School of Geographic and Oceanographic Sciences, Nanjing University, Nanjing 210093, China
[b] Key Laboratory of Coast and Island Development (Nanjing University), Ministry of Education, Nanjing 210093, China
[c] Marine Fisheries Research Institute of Jiangsu Province, Nantong 226007, China

HIGHLIGHTS

- PAHs are important indicators of anthropogenic activities on the environment.
- PAHs levels in the Yangtze River Estuary and adjacent coastal areas were studied.
- Kriging interpolation and PMF model used to study spatial distribution and sources.
- Anthropogenic activities were the main sources of PAHs in the study area.
- Distribution patterns influenced by factors like sediment size and hydrodynamics.

ARTICLE INFO

Article history:
Received 5 May 2016
Received in revised form
15 July 2016
Accepted 24 July 2016
Available online 30 July 2016

Handling Editor: Caroline Gaus

Keywords:
Polycyclic aromatic hydrocarbons
Surface sediment
Source apportionment
Yangtze River Estuary
Anthropogenic activities
Marine dynamics

ABSTRACT

Polycyclic aromatic hydrocarbons (PAHs) are mainly produced by incomplete combustion and are used as indicators of anthropogenic activities on the environment. This study analyses the PAHs level in the Yangtze River Estuary (YRE), an important component of Yangtze River and a developed and populated region in China. Surface sediments were collected from 77 sites at the YRE and its adjacent coastal zone (IACZ) for a comprehensive study of PAHs. Kriging interpolation technology and Positive matrix factorization (PMF) model were applied to explore the spatial distribution and sources of PAHs. Concentrations of 16 PAHs (ΣPAHs) varied from 27.2 ng g^{-1} to 621.6 ng g^{-1} dry weight, with an average value of 158.2 ng g^{-1}. Spatially, ΣPAHs exhibited wide fluctuation and exhibited an increasing tendency from north to south. In addition, ΣPAHs exhibited a decreasing trend with increasing distance between the estuary and IACZ. The deposition flux of PAHs indicated that more than 107.8 t a^{-1} PAHs was deposited in the study area annually. The results of the PMF model revealed that anthropogenic activities were the main sources of PAHs in the study area. Vehicle emissions and marine engines were the most important sources and accounted for 40.9% of the pollution. Coal combustion, petrogenic sources, and wood combustion were other sources that contributed 23.9%, 23.6%, and 11.5%, respectively. The distribution patterns of PAHs in the YRE and IACZ were influenced by many complicated factors such as sediment grain size, hydrodynamics and so on.

1. Introduction

Polycyclic aromatic hydrocarbons (PAHs) are typical persistent organic pollutants that have attracted scientific and regulatory interests due to their toxic, carcinogenic, and mutagenic properties (Sverdrup et al., 2002; Qiao et al., 2006; Zhang and Tao, 2009). They mainly originate from anthropogenic activities such as incomplete combustion of fossil fuels, biomass burning, coke ovens, and exhaust emissions (Yunker et al., 2002; Simoneit, 2002). Natural processes such as oil seeps, forest fires, and organic matter

* Corresponding author. School of Geographic and Oceanographic Sciences, Nanjing University, Xianlin Avenue 163, Nanjing 210023, China.
E-mail address: zouxq@nju.edu.cn (X. Zou).

http://dx.doi.org/10.1016/j.chemosphere.2016.07.075
0045-6535/

diagenesis can also act as significant sources (Simoneit, 2002; Lima et al., 2005). PAHs are transported to marine ecosystems through direct and indirect pathways including atmospheric deposition and riverine inputs (Wang et al., 2007; Lin et al., 2013). Following release into the marine environment, most PAHs are easily adsorbed onto the surface of fine particles and are eventually deposited into the underlying sediments due to their high hydrophobicity and lipid solubility (Kim et al., 1999; Li et al., 2006, 2012). Therefore, marine environment, especially marginal sea is an important reservoir of PAHs.

Estuarine areas are important component of the river and the marginal sea, and serve as a transition zone between seawater and freshwater. Therefore, the hydrodynamic conditions and biodiversity are always complex in estuarine regions (Yu et al., 2015). River discharge and sedimentary processes influence the distribution and behavior of PAHs in estuarine-coastal environments (Lin et al., 2013). In addition, transport and storage of terrestrial organic materials in these zones, especially large-river delta-front estuaries, are significant due to interactions of several physical, chemical, and biological processes (Bianchi and Allison, 2009; Hung et al., 2011; Liu et al., 2012). Therefore, estuarine-coastal areas are important sinks of PAHs from the atmosphere and land. The Yangtze River Estuary (YRE), a typical estuary in the East China Sea (ECS), is one of the most prosperous regions in China and receives significant amounts of sediments and runoff from the river basin. Additionally, the YRE also acts as a conduit discharging large amount of organic pollutants including PAHs, which originate from intensive industrialization and urbanization in the basin, into the ECS. Therefore, more attention should be paid to the comprehensive study of the sources, compositions, distribution patterns, and environmental behavior of the PAHs in the YRE.

To date, several studies have investigated PAHs distribution in the YRE (Li et al., 2012; Lin et al., 2013; Yu et al., 2015), focusing on the sources, compositions, and distributions of PAHs. However, few studies have discussed influencing mechanisms such as hydrodynamic conditions and granularity effects (Lin et al., 2013). In addition, previous studies primarily focused on the Yangtze River subaqueous delta, and limited attention was paid to its adjacent coastal zones (IACZ). Fig. 1c highlights the demarcation of IACZ from the YRE, using a hypothetical line between the YRE and Hangzhou Bay. We called the north of this line as the YRE and the south of this line as IACZ. Numerous studies have demonstrated that transport of sediments from the Yangtze River to the ECS is controlled by tidal currents, shallow sea circulations, Changjiang estuarine circulations, and storm events (Gao et al., 2011; Milliman et al., 1984; Su and Wang, 1986). Under the influence of complex hydrodynamic conditions, a large amount of fine particles discharged by the river are transported southwards and formed two mud deposition centers: one outside the YRE and Hangzhou Bay named as the YRE mud area (YREMA) and the other along the Zhe-Min coast named as the Zhe-Min Coastal mud area (ZMCMA) (Qin et al., 1987; DeMaster et al., 1985; Liu et al., 2007) (Fig. 1b). Therefore, the distribution patterns of PAHs in these regions under the effect of ocean currents (e.g., the Yellow Sea Coast Current and the Taiwan Warm Current (TWWC)) and the reduction of river runoff will be distinct. In addition, other factors such as anthropogenic activities and granularity effect were also taken into account in this study to explore the behavior of PAHs in the YRE and IACZ.

This paper focuses on the concentration, composition, and distribution patterns of the PAHs in the YRE and IACZ. Spatial interpolation technology and the Positive Matrix Factorization (PMF) method were applied to quantify the distribution patterns and sources of PAHs based on 77 samples. The objectives of this study were: 1) to investigate the sources, composition, and spatial distribution of the PAHs in the YRE and IACZ; 2) to examine the role of granularity effect, hydrodynamic conditions, and anthropogenic activities on PAHs levels in the sediments.

2. Materials and methods

2.1. Study area and sample collection

The Yangtze River is the longest river (6300 km) in Asia, globally ranking fifth in water discharge levels and fourth in sediment loads, measuring at 920 km^3 a^{-1} and 480 million tons a^{-1}, respectively (Milliman and Syvitski, 1992; Yang et al., 2006). The Yangtze River Basin is one of the most prosperous regions in China hosting developed cities such as Chengdu, Chongqing, Wuhan, Hefei, Nanjing, Suzhou, Wuxi, and Shanghai. It is populated by 400 million inhabitants and has a drainage area of 1.8×10^6 km^2 accounting for nearly 20% of the mainland (Yang et al., 2006). Intensive industrialization and urbanization in the basin have resulted in large amounts of organic pollutants including PAHs being discharged into the river (Qi et al., 2014). The YRE, one of the most urbanized and industrialized regions, is a key shipping hub connecting inland and the ECS (Zhou et al., 2014). The YRE acts as a conduit, discharging large amount of sediments from the river basin into the estuary, forming a large-scale subaqueous delta and mud area (YREMA and ZMCMA) (Fig. 1b). Over half of these discharged sediments and PAHs are trapped in the YRE due to coastal currents (Liu et al., 2007; Li et al., 2012; Lin et al., 2013). Several studies have focused on the flux of PAHs discharged into the ECS. Wang et al. (2007) estimated that the annual flux of the 16 USEPA priority PAHs from the Yangtze River to the ECS was 232 t. Qi et al. (2014) estimated that more than 369 t PAHs were discharged into the ECS annually through the Yangtze River making it one of the largest contributors of PAHs to the western Pacific shore. Therefore, pollutant load of PAHs will pose an increasing burden to water security and health of the marine coastal ecosystem (He et al., 2011; Qi et al., 2014).

In this study, we focus on the YRE and IACZ which located at the north of ZMCMA as the study area. The study area was divided into 13 vertical sections and 77 compartments with sampling sites located in the center of each compartment. The sampling sties were uniformly distributed as highlighted in Fig. 1c. Surface sediment samples (at 0–2 cm depth) were collected from each site using stainless steel grab samplers, during December 2013. All samples were placed in pre-cleaned aluminum foil and stored at −20 °C prior to analysis.

2.2. PAHs analysis

A standard mixture solution consisting of 16 priority PAHs namely naphthane (Nap), acenaphthylene (Acy), acenaphthene (Ace), fluorene (Flu), anthracene (Ant), phenanthrene (Phe), benzo[*a*]anthracene (BaA), chrysene (Chr), fluoranthene (Flo), pyrene (Pyr), benzo[*a*]pyrene (BaP), dibenzo[a,h]anthracene (DahA), benzo[*b*]fluoracene (BbF), benzo[k]fluoracene (BkF), benzo[g,h,i]perylene (BghiP), and indeno[1,2,3-*cd*]pyrene (IcdP) was obtained from Supelco (Bellefonte, PA, USA) and used for external calibration. All solvents (dichloromethane, acetone, and n-hexane) used during the processing were HPLC grade (Tedia Co. Inc., USA). Analytical grade anhydrous sodium sulfate was activated at 450 °C for 5 h to remove impurities before use. Silica gel (100–200-mesh particle size; Qingdao Haiyang Chemical Co. Inc., Shandong, China) was extracted using acetone, dichloromethane, and n-hexane, and activated for approximately 16 h at 130 °C.

PAHs extraction was performed as described by Yim et al. (2014) and Wang et al. (2015). Sediments were freeze-dried and then sieved through an 80-mesh sieve. A 5 g surface sediment sample

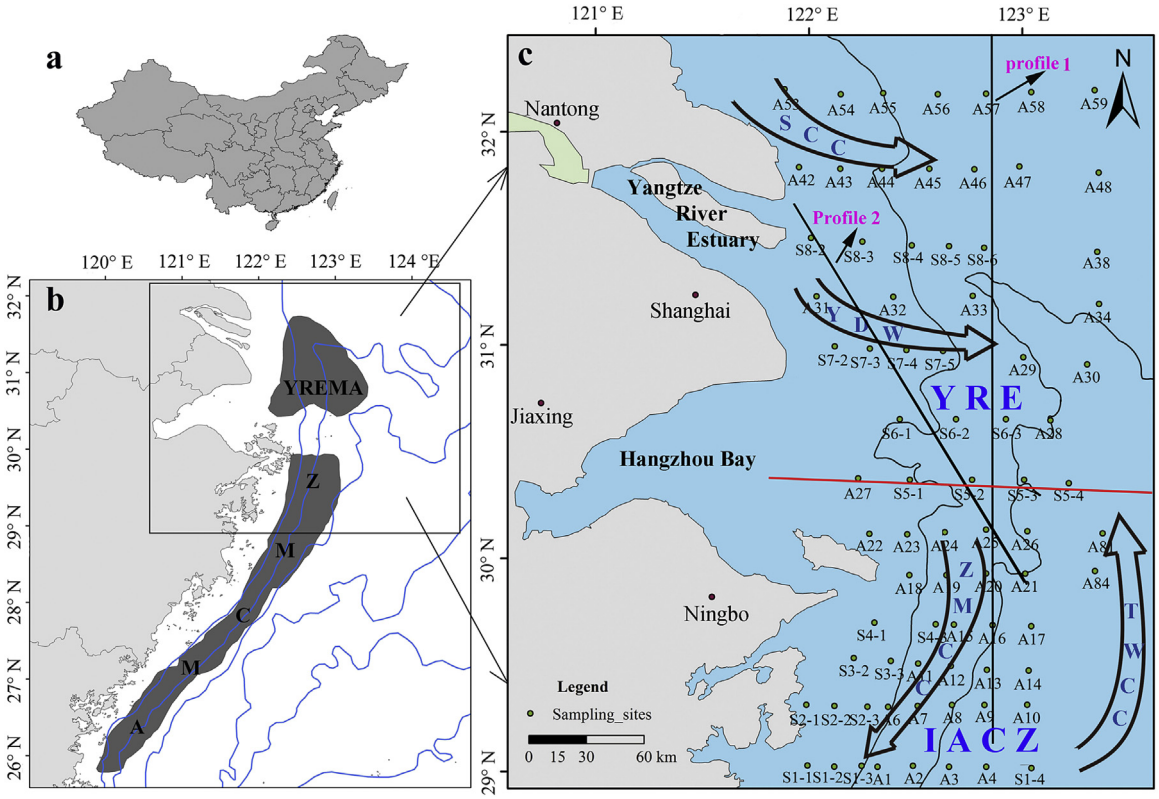

Fig. 1. Map showing sediment-sampling sites in the Yangtze River Estuary and its adjacent coastal zone (YREMA: the Yangtze River Mud Area; ZMCMA: the Zhe-Min Coastal Mud Area; SCC: Subei coastal current, YDW: Yangtze River diluted water, ZMCC: Zhe-Min coastal current, TWCC: Taiwan warm current).

was Soxhlet-extracted using 100 mL n-hexane/acetone (1:1 v/v) for 24 h, and 2 g activated copper was added for desulphurization. The extracted solution was concentrated to 1–2 mL in a rotary evaporator, and cleaned using a chromatography column (25 cm × 1 cm internal diameter) with 5 g silica gel and 2 cm anhydrous sodium sulfate. The concentrated solution was added to the column and eluted with 50 mL n-hexane/dichloromethane (3:2 v/v). The eluate containing the PAHs was vacuum-evaporated and solvent-exchanged with n-hexane, and finally concentrated to 1 mL under a gentle stream of nitrogen.

A Shimadzu QP2010 Ultra GC/MS equipped with a fused silica capillary Rtx-5MS column (30 m × 0.25 mm internal diameter, 0.25 μm film thickness) was used to determine the concentration of PAHs. Helium was used as carrier gas with a flow rate of 1.0 mL min^{-1}. The GC temperature model was as follows: an initial temperature of 80 °C was held for 2 min and increased at a rate of 20 °C min^{-1} to 180 °C and held for 5 min. Then, it was increased at a rate of 10 °C min^{-1} to 290 °C and held for 15 min. The injection port was set at 290 °C. Subsequently, 1 μL of the sample extract was injected in the split-less mode. The interface and ion source temperatures were maintained at 290 °C and 230 °C, respectively. The ionization was carried out in the electron impact mode at 70 eV and data was acquired using selective ion monitoring mode.

A procedural blank and a matrix-spiked samples consisting of all the analytes were analyzed with every six-sample set. Duplicates were run every 12 samples and samples were reanalyzed if the difference exceeded by more than 15%. The AHs were quantified using the external standard method effectively demonstrated by Wang et al. (2015). Calibration curves based on sets of five standard concentrations of 10 ng L^{-1}, 50 ng L^{-1}, 100 ng L^{-1}, 250 ng L^{-1}, and 500 ng L^{-1} were drawn. The standard curve was checked every day using the reference standard to ensure satisfactory linear regression coefficients ($R^2 > 0.999$) for all PAHs tested. The average recoveries of PAHs based on the matrix-spiked samples ranged from 74.5% to 106.2%. Limit of detection was calculated as three times the noise level of the blank sample (Wang et al., 2015) and ranged between 0.16 ng g^{-1} to 0.77 ng g^{-1} for all the analytes.

2.3. Positive matrix factorization (PMF) for source apportionment

The PMF model is a powerful and widely useful factorization method for source apportionment and does not need source profile data (Zhang et al., 2012) in comparison to other receptor models like chemical mass balance model. The model, developed in 1994, is an advanced method of multivariate factor analysis based on weighted least squares (Paatero and Tapper, 1994). The PMF is particularly suitable for environmental data because it accounts for variable uncertainties and constrains all values to be positive, as in real environmental problems (Comero et al., 2014). Details of the PMF model are described in EPA PMF 5.0 Fundamentals & User Guide (US EPA, 2014). In principle, the PMF model can be described by the following equation:

$$x_{ij} = \sum_{j=1}^{p} g_{ik} f_{kj} + e_{ij} \quad (1)$$

where, x_{ij} is the ith species concentration determined by the jth sample; g_{ik} is the ith species concentration measured in the kth source; f_{kj} is the kth source contribution to the jth sample; and e_{ij} is the error of the models for the species j measured in sample i (Hopke, 2003). The model is obtained by minimizing the objective function $Q(E)$ through an iterative algorithm as shown in equation (2).

$$Q(E) = \sum_{i=1}^{n}\sum_{j=1}^{m}\left[\left(x_{ij} - \sum_{k=1}^{p} g_{ik}f_{kj}\right)\Big/ s_{ij}\right]^2 \quad (2)$$

where, $Q(E)$ is the weighted sum of squares of differences between the PMF output and the original data set (Lin et al., 2013); and s_{ij} is the uncertainty in the jth PAH for ith sample (US EPA, 2014). Details of s_{ij} can be found in literature (Lin et al., 2013; Yu et al., 2015).

Uncertainly file should be required in the model to estimate the confidence level for each value, and all values of concentration and uncertainly file should be positive. Therefore, the data below detection limits was replaced with half part of detection limits. In the present study, values of uncertainly matrix were calculated by equation in the User Guide (US EPA, 2014).

2.4. Deposition flux

Deposition flux of PAHs in the surface sediments was estimated to assess the extent of contamination and their potential toxicity as a pollution source. The deposition flux was calculated using several sediment properties and PAHs concentration, as shown in equation (3).

$$F_{deposition} = A \cdot C_{PAHs} \cdot \rho \cdot \omega \cdot (1 - \varnothing) \quad (3)$$

where, A is the area of a given region (km^2), C_{PAHs} is the measured sedimentary PAHs concentration (ng g^{-1}), ρ is the dry density of the sediment samples (g cm^{-3}), ω is the sedimentation rate (cm a^{-1}), and $\varnothing$ is the sediment porosity (dimensionless). $\varnothing$ is a widely measured value in sediment mixing layers around the world and ranges from 0.7 to 0.8 (Ali et al., 2014; Fang et al., 2015). We selected a median value of 0.75 to represent sediment porosity in the study area. A recommended value of 1.2 g cm^{-3} was selected for ρ (Liu et al., 2007). The Kriging interpolation method was used to obtain the spatial distribution of ω based on accurately dated values collected in the study area (Su and Huh, 2002; Wang, 2003; Duan et al., 2005; Zhang et al., 2009; Wang et al., 2013).

Grain-size analysis, as described by Liu et al. (2014), was conducted. Briefly, the surface sediment samples were dispersed in sodium metaphosphate for 24 h and vibrated in ultrasonic for 30 s to ensure full dispersion. Samples were analyzed using a Malvern 2000 laser diffraction particle sizer with a measurement range of 0.02 μm–2000 μm. Particle size parameters including mean, sorting coefficient, and skewness were calculated using specific formulas (Mcmanus, 1988).

3. Results and discussion

3.1. Spatial distribution and composition of PAHs in surface sediments

The total concentration of the 16 PAHs (ΣPAHs) in the sediments from the 77 sites varied from 26.6 ng g^{-1} to 621.6 ng g^{-1}, with an average value of 158.2 ng g^{-1}. Weights of PAHs were expressed as dry weight. A comparison with results from other studies is listed in Table S1 (Supplement Material). In this study, PAHs concentration was relatively high compared to the study by Lin et al. (2013) and was relatively close to the results from Li et al. (2012) and Yu et al. (2015). However, PAHs concentration in this study was low to moderate compared to other large estuarine-coastal zones such as Pearl River Estuary (Chen et al., 2006), Nile Estuary (Barakat et al., 2011), Guan River Estuary (He et al., 2014), and Yellow River Estuary (Qin et al., 2011) (Table S1). The middle and lower reaches of the Yangtze River is near highly developed regions accounting for large amounts of PAHs discharge into the estuary that could have been diluted by large volumes of runoff and sediment loads (Lin et al., 2013). Spatially, PAHs concentration presented a wide fluctuation, and exhibited an increasing tendency from north to south (Fig. 2a and Fig. 3a). The lowest and highest concentrations were located at sites A58 and A20, respectively. To understand the trend in variation of PAHs from north to south in detail, we utilized ProfileGraph technology in ArcGIS 10.0 to acquire the value of PAHs in profile 1 (Fig. 1c). Fig. 3a highlights the concentration gradient of PAHs from north to south, which shows the concentration of PAHs in profile 1. In addition, ΣPAHs tended to decrease with increasing distance between the estuary and the sea, as demonstrated by Li et al. (2012). This progressive decreasing trend has also been confirmed in previous studies on terrigenous pollutants in the ECS, such as heavy metals (Lin et al., 2002), short chain chlorinated paraffins (Zeng et al., 2012), nonylphenol, and bisphenol A (Bian et al., 2010). We also set a profile (profile 2) from the estuary to coastal ocean (Fig. 1c) to explore the variation of PAHs. Obviously variation trend of PAHs in Fig. 3b indicates that the PAHs were high in the estuary and were lower away from estuary, and eventually become high further in the coastal ocean. Detailed interpolations on the concentration fluctuations have added in the revised manuscript (shown in Fig. 3a and b). Therefore, terrestrial pollutants discharged through the Yangtze River are probably the primary pollution sources in the YRE. Fig. 2a highlights that the distribution pattern of sedimentary PAHs in our study area can be divided into two partitions: the YRE and IACZ. The ΣPAHs in the YRE ranged from 27.2 ng g^{-1} to 400.9 ng g^{-1}, with an average value of 137.7 ng g^{-1}, which is relative lower than the level of PAHs in the IACZ (ranged from 27.3 ng g^{-1} to 621.6 ng g^{-1}, with an average value of 175.8 ng g^{-1}). In addition, a similar trend was also found at the aspect of grain-size which tended to be finer as we moved from north to south (Fig. 3c). The YRE is an important shipping hub and shipping activity frequently results in large oil spills that contribute to relatively high levels of PAHs in this estuary. Fig. 2a shows that PAHs accumulation was dominant in the south of IACZ and not in the YRE. The distribution pattern of PAHs in this study was very similar to previous results (Lin et al., 2013) that indicated that most sediment-associated PAHs trapped in the YRE were re-suspended by the East Asian winter monsoon storms and transported by the southbound Zhe-Min Coastal Current (ZMCC) to the ZMCMA.

PAHs can be divided into two groups: low-molecular-weight PAHs (LMW PAHs with 2–3 rings) and high-molecular-weight PAHs (HMW PAHs with 4–6 rings), based on the number of benzene rings. In this study, the concentration of LMW PAHs ranged from 2.5 ng g^{-1} to 185 ng g^{-1}, which accounting for 9.2%–69.6% of ΣPAHs, with an average value of 37.7%. The concentration of HMW PAHs was relatively high and ranged from 12.9 ng g^{-1} to 436.3 ng g^{-1}, and accounted for 30.3%–89% of ΣPAHs, with an average value of 62%. The concentration of HMW PAHs was relatively higher than LMW PAHs in the study area, probably due to their physicochemical properties. Previous studies have demonstrated that HMW PAHs can exist for long periods in ambient environmental conditions and are easily absorbed onto the surface of fine particles (Lin et al., 2013; Li et al., 2015). Fig. 4 illustrates the distribution patterns of LMW PAHs and HMW PAHs in the study area. In general, LMW PAHs and HMW PAHs were mainly concentrated in the YRE and the south part of IACZ, and tended to decrease with increasing distance between the estuary and IACZ. The composition of PAHs in the YRE and IACZ exhibited significant difference. In the YRE, the concentration of LMW PAHs ranged from 2.5 ng g^{-1} to 136.87 ng g^{-1} with an average value of 53.56 ng g^{-1}, and HMW PAHs ranged from 23.86 ng g^{-1} to 264.07 ng g^{-1} with an average value of 83.83 ng g^{-1}. In IACZ, the concentration of LMW PAHs ranged from 8.3 ng g^{-1} to 185.3 ng g^{-1} with an average value

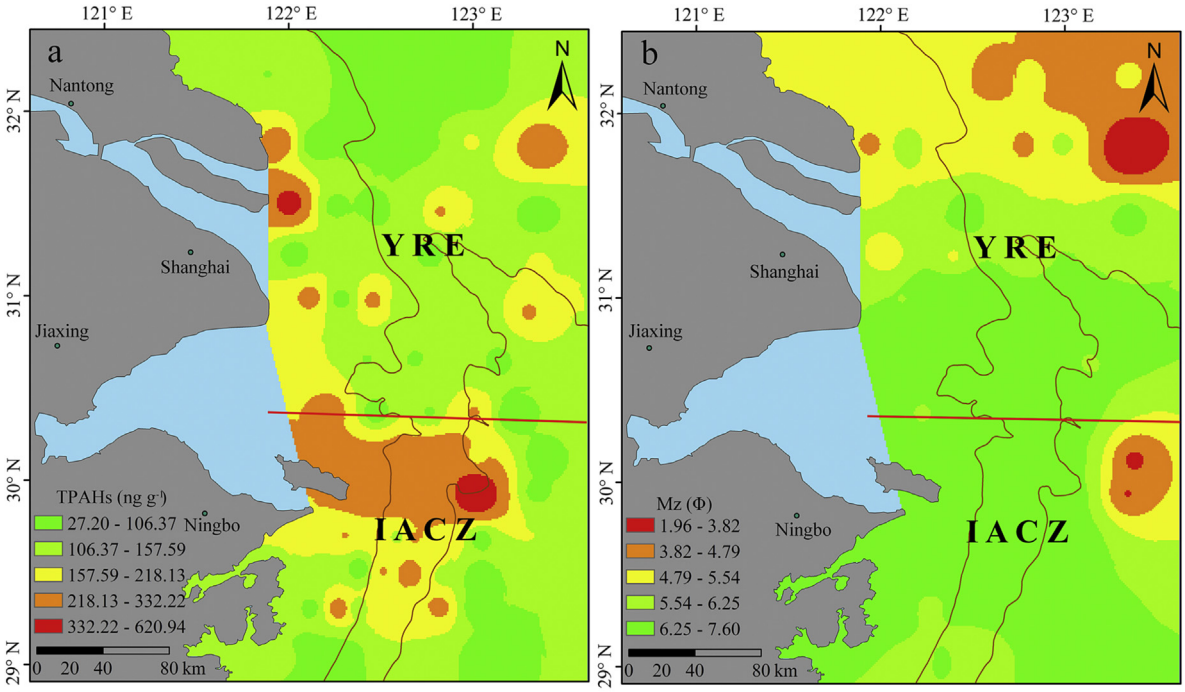

Fig. 2. Distribution patterns of ΣPAHs and grain-size in surface sediments of the YRE and IACZ.

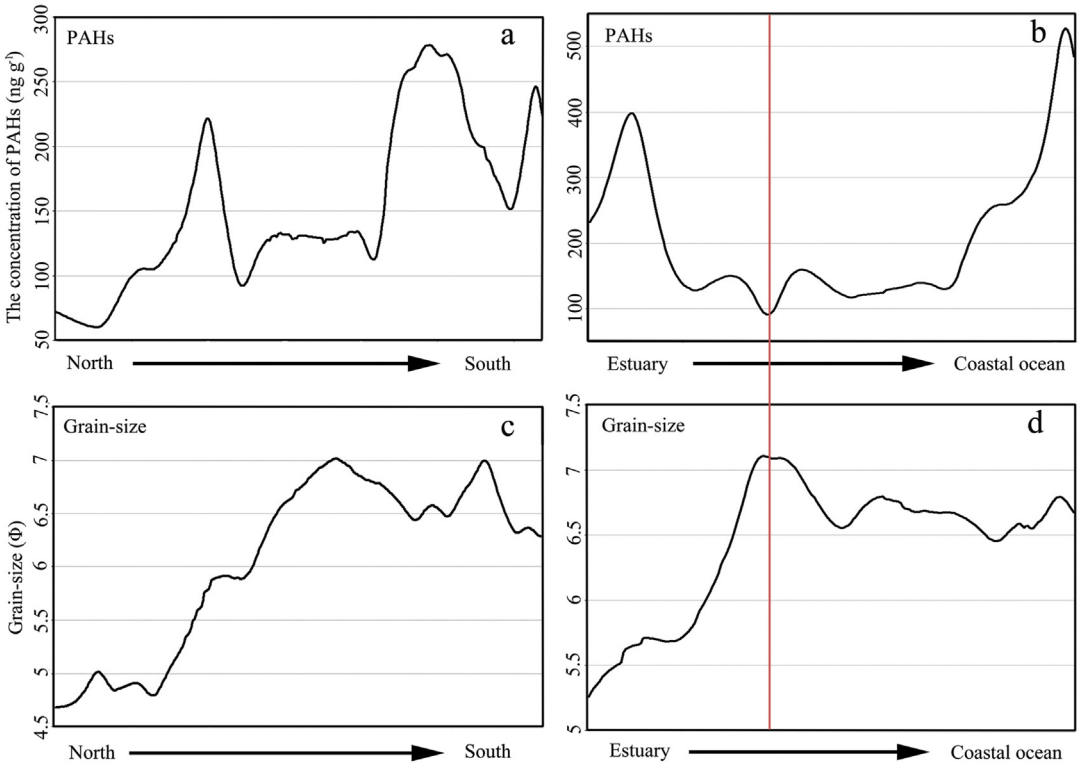

Fig. 3. ProfileGraph value of PAHs and sediment grain-size in Sections 1 and 2.

of 63.18 ng g^{-1}, and HMW PAHs ranged from 12.9 ng g^{-1} to 436.28 ng g^{-1} with an average value of 112.4 ng g^{-1}. Overall, the concentration of HMW PAHs in IACZ was relatively higher than the YRE, but the concentration of LMW PAHs in the YRE was similar to IACZ.

Previous studies have demonstrated that petroleum mixtures containing high level of LMW PAHs and HMW PAHs are generated from high temperature combustion sources such as biomass burning, fossil fuel combustion, and vehicles emissions (Yunker et al., 2002). High level of LMW PAHs in the estuary may have

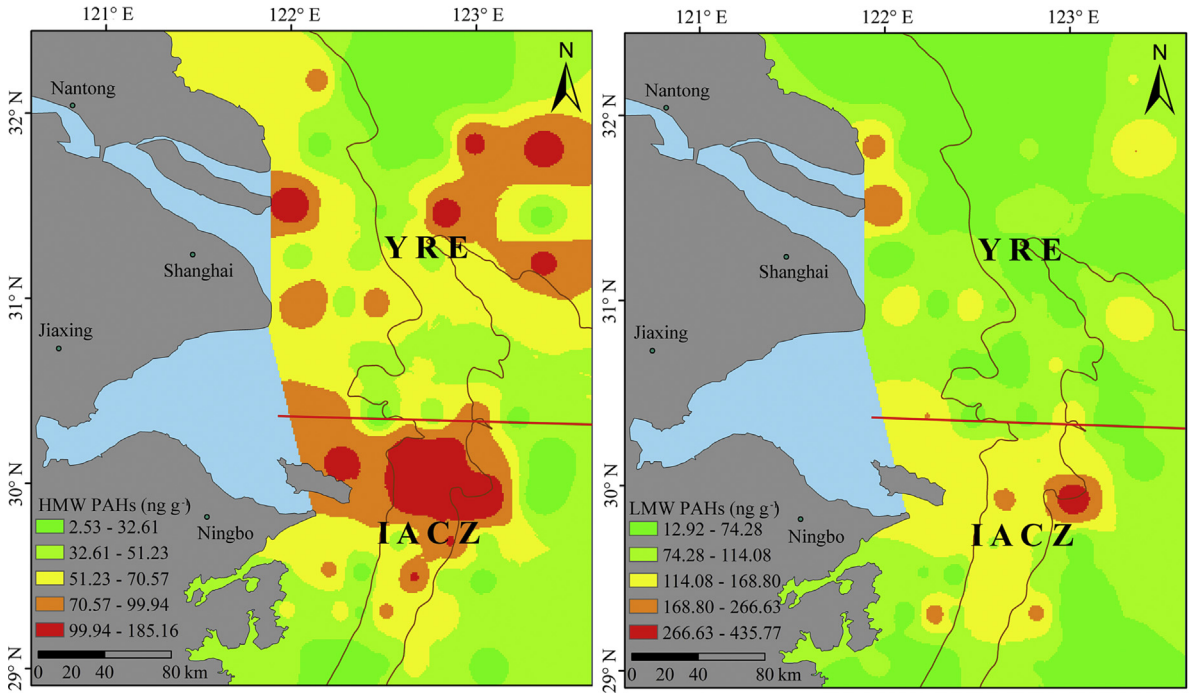

Fig. 4. Distribution patterns of HMW PAHs and LMW PAHs in the YRE and IACZ.

also been caused by oil leaks due to shipping activity. The ratio of LMW/HMW was used as an index to qualitatively interpret the sources of PAHs, where a ratio higher than 1 indicated a petrogenic source and the ratio lesser than 1 indicated a pyrogenic source (Li et al., 2015). In the present study, the ratio of LMW/HMW at most sites was lower than 1 (Fig. 5) indicating that pyrogenic sources were dominant in the YRE. Therefore, anthropogenic activities may be the main sources of sedimentary PAHs in the YRE and IACZ. The middle and lower reaches of the Yangtze River are the most developed and populated regions hosting two of the five major metropolitan areas: the Yangtze River Delta metropolitan area and the metropolitan area in the middle reaches of the Yangtze River. In 2014, the region had over 320 million inhabitants and the Gross Domestic Product (GDP) of these two metropolitan areas was 20 trillion CNY accounting for 31.4% of the national GDP (National Bureau of Statistics of China, 2014). According to preliminary estimations, about 9.3 $\times$ 10^3 t PAHs was emitted into the environment by the provinces along the Yangtze River, which accounted to 36.6%

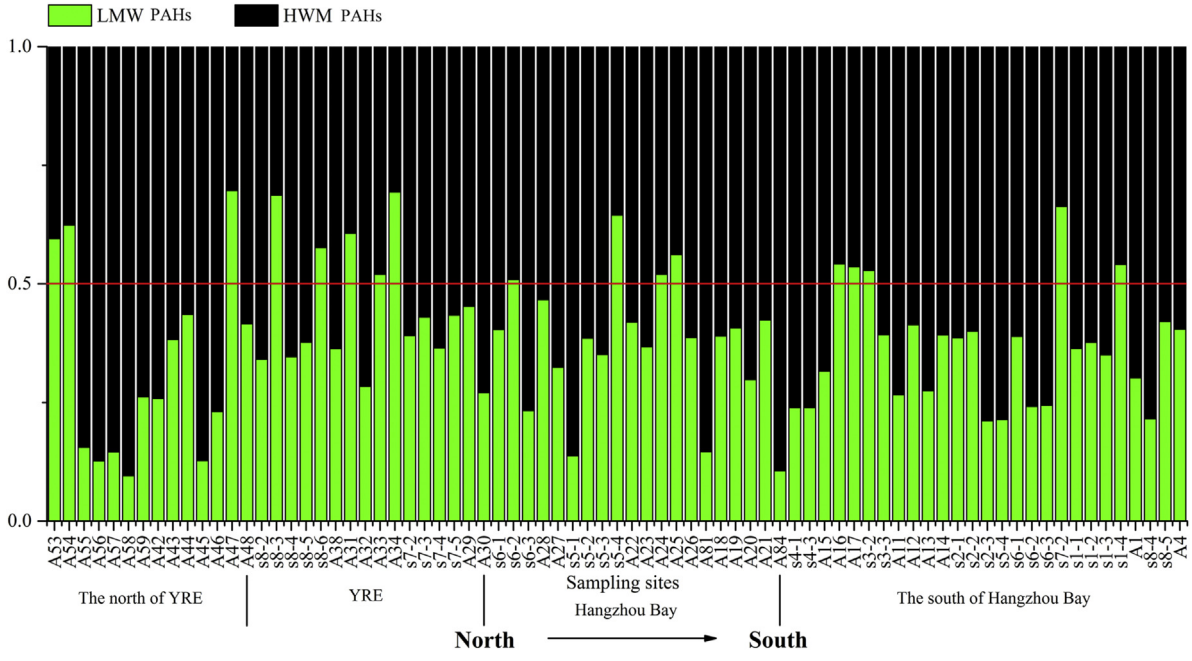

Fig. 5. Variation of HMW/LMW ratios from north to south.

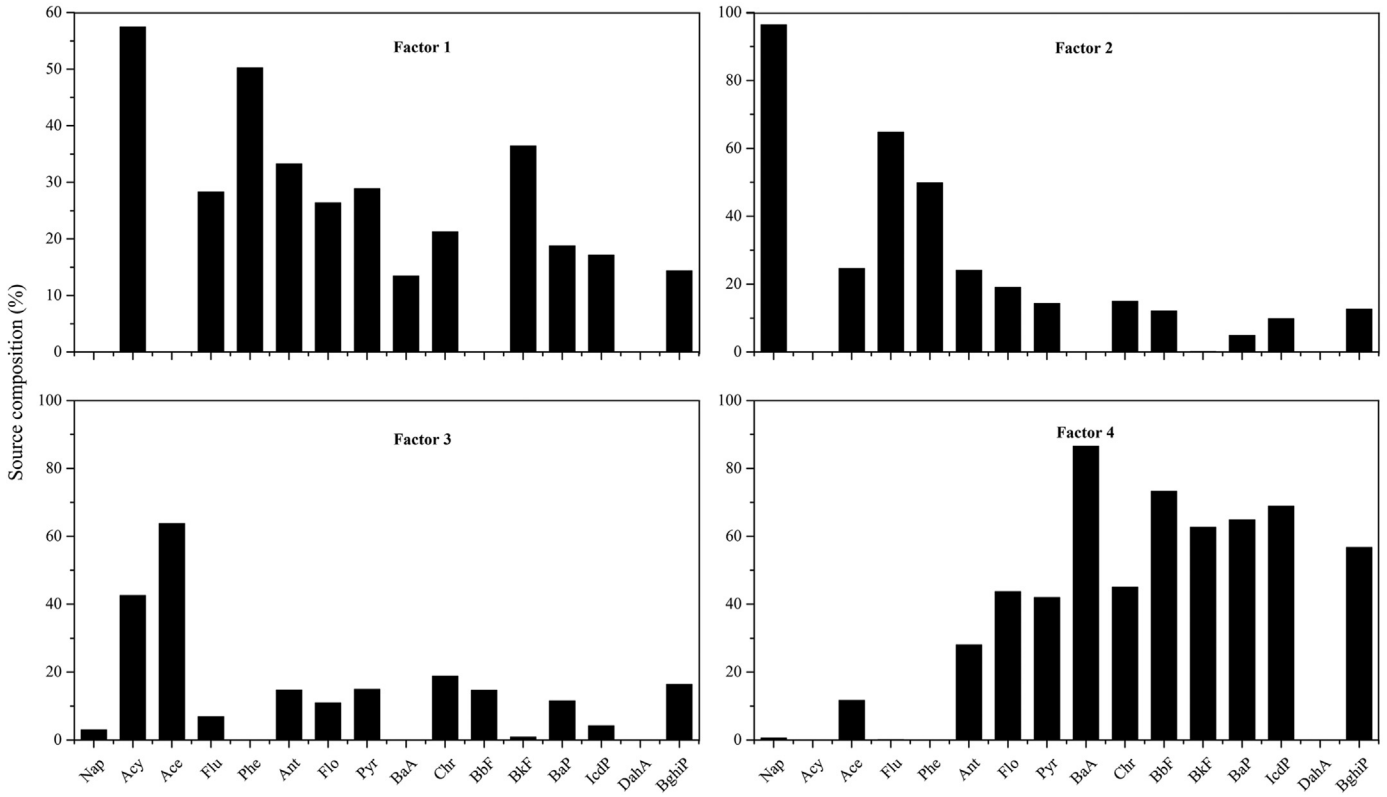

Fig. 6. Source compositions of PAHs in four factors obtained using PMF model in the YRE and IACZ.

of the national emissions (Huang and Zhang, 2015). There were nearly 279 million motor vehicles, with nearly 172 million cars (Traffic Management Bureau of The Public Security Ministry, 2015). In addition, over 200 million cars were operational in 11 cities (i.e. Beijing, Chengdu, Shenzheng, Shanghai, Chongqing, Tianjin, Suzhou, Zhengzhou, Hangzhou, Guangzhou, and Xi'an), and nearly half of them were located in the Yangtze River Basin (Traffic Management Bureau of The Public Security Ministry, 2015). Thus, fossil fuel consumption and exhaust gas emissions were high.

3.2. Apportionment of PAHs' sources in surface sediments

As composition of PAHs from anthropogenic and natural sources overlap, source apportionment of PAHs was executed with attention. PMF model was used in this study to identify the possible sources of PAHs in the sediment samples from the YRE and IACZ.

A 77 × 16 dataset (77 samples and 16 PAH species) was introduced into the EPA PMF 5.0 model to estimate the contributions of various sources. A robust model was adopted to eliminate the effect of individual extreme values, and DahA was excluded from the matrix due to its low signal-to-noise (S/N) ratio. The PMF model was executed with 3–6 factors, each individually initialized with different starting points (Lin et al., 2013). The 4-factor solution had a calculated value of Q at 782, and was closest to the theoretical value of 860 (calculated by equation $Q = i \times j - p \times (i + j)$) (Tian et al., 2015; Shi et al., 2009, 2016). Therefore, four factors, each explaining percentage contributions of various PAHs, were finally extracted using the PMF model (Fig.6). Factor 1 accounted for 23.9% of the total factor contribution was highly loaded by Phe, BkF, and BaA. Phe and BkF are identified as good indicators of coal combustion (Simcik et al., 1999; Sofowote et al., 2008). Factor 2 accounted for 23.6% of the total factor contribution and was loaded predominantly by Nap and moderately by Flu and Phe. Nap has previously been demonstrated as a possible proxy of petroleum spill (Liu et al., 2009), stipulating that factor 2 may represent a petrogenic source. Factor 3 contributed 11.5% of the total factor contribution and was highly loaded by Acy and Ace. Acy, a LMW PAHs, is considered as an important indicator of wood combustion (Khalili et al., 1995). Factor 4 explained 40.9% of the total factor contribution and was consistent with vehicle emissions indicating a significant contribution from HMW PAHs such as BbF BaP, Chr, IcdP, and BghiP. Previous studies have demonstrated that IcdP mainly originates from diesel emissions (Simcik et al., 1999; Li et al., 2003) and BghiP can be used as a tracer of gasoline emissions (Simcik et al., 1999; Wang et al., 2009). Therefore, factor 4 was selected to represent gasoline and diesel emissions that originated from vehicle emissions and marine engines. PMF model was successfully used in a previous study for quantitative source apportionment of sedimentary PAHs in the YRE (Yu et al., 2015). Three sources were successfully identified: gasoline and fossil fuel combustion (source 1), coke plant emissions and biomass combustion (source 2) and petrogenic sources (source 3), which were quite similar to our study (Yu et al., 2015). Additionally, we successfully identified coal combustion source and wood combustion source increasing reliability of our results.

3.3. Assessment of fate and transport mechanisms of PAHs

3.3.1. Role of sediment grain-size on the distribution of PAHs

The granulometric composition of the sediments from the YRE and IACZ are summarized in Fig. 2b. Distribution pattern of the granulometric composition was coarse in the north of the YRE and fine southward. Coarsest particles with grain size of 1.95 Φ were located at site A48 and the finest particles with grain size of 7.6 Φ.

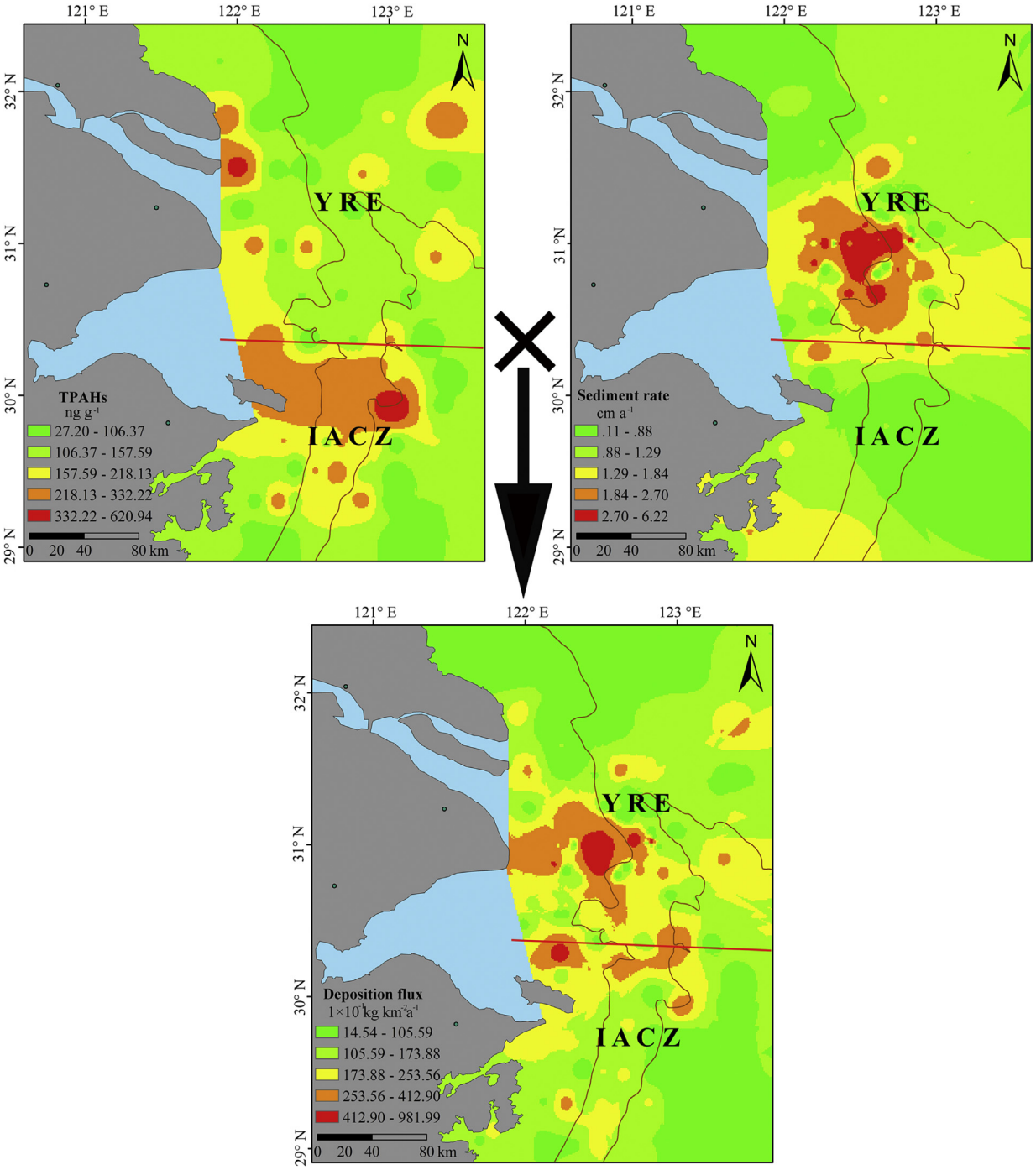

Fig. 7. Deposition patterns of sedimentary PAHs in YRE and IACZ.

were located at site S7-4. The sediments in the north of the YRE consisted largely of sand with a median grain size of 4.76 Φ, and the sand content ranged from 8.6% to 100% with an average value of 46%. On the contrary, the sediments in the southern part mainly comprised of mud components (silt and clay) and ranged from 77.2% to 100% with a mean value of 94.3%. In general, grain-size in the study area displayed a decreasing trend from north to south, which corresponded with the increasing trend of PAHs concentration. Fig. 3 displays the PAHs concentration and grain-size of the two sections, and helps us understand the variation in PAHs concentration and grain-size in the study area. The variation trend of PAHs concentration and grain-size from north to south (Fig. 3a,c) is more consistent, but the variation of granularity is more conspicuous. Fig. 3b,d depict the variation trend of PAHs concentration and grain-size from estuary to the remote sea. Viewed as a whole, the variation trend of these indexes was not consistent. However, we find that the variation trend of PAHs concentration and grain-size near the estuary are more consistent (shown in Fig. 3b,d; on the left side of the red line). In the remote sea, the sediment grain-size tended to be uniform and PAHs concentration was mainly controlled by the regional marine dynamics. Linear regression was carried out between sediment concentrations of ΣPAHs, individual

PAHs, and mean grain size to further demonstrate our viewpoint. However, the results of linear regression showed that the relationship between ΣPAHs and individual PAHs did not exhibit significant correction with mean grain size (not shown here). This result seems to indicate that there was no relationship between PAHs content and sediment grain size, and was in contradiction to the above conclusion. Nevertheless, we think that factors that influence PAHs concentration in the YRE and IACZ are complicated, and were not controlled only by the sediment grain-size. In addition, hydrodynamics, organic contents, partition coefficients and so on, may also influence the fate of PAHs and contribute to low correlation between PAHs content and the sediment grain size.

3.3.2. Role of hydrodynamic forcing on the PAHs dispersal and preservation

Fig. 1c depicts the complex hydrodynamic conditions that control distribution patterns of the sediments and associated PAHs in our study area, including the Yangtze Diluted Water (YDW) or the Yangtze River runoff, Subei Coastal Current, ZMCC, and TWWC (Liu et al., 2007; Gao and Wang, 2008). Previous studies have demonstrated that the sediments and associated PAHs are highly concentrated in the YRE and the inner shelf of the ECS, owing to the hydrodynamic conditions in this area (Lin et al., 2013; Yu et al., 2015). During flood season (May to October), more than 80% of the mean annual sediments of the Yangtze River was discharged into the YRE (Guo et al., 2007) with YDW, which lead to the difference between short and long-term deposition rates (~4 cm mo^{-1} in the flood season and ~1–5 cm a^{-1} in the long-term) (Liu et al., 2006). Therefore, a large amount of the river-derived sediment is eroded seasonally and is transported southward along the coastal area of Zhejiang and Fujian Provinces (Liu et al., 2006) and forms alongshore deposits which are named as ZMCMA (Fig. 1b). Meanwhile, large amounts of PAHs bound to the sediment were also discharged into the YRE and eventually deposited in the underlying sediment. Therefore, the YRE is a deposition center of PAHs. However, YDW was very strong and could reach 200 km from the river mouth (Gao et al., 2000) in the flood season, which may have diluted the water mass in this area and lead to the decreasing trend of PAHs from the river mouth to the IACZ (Gao and Wang, 2008; Lin et al., 2013) (Figs. 2a and 3b). Meanwhile, the southeast monsoon prevalent in the summer in this area, which intensifies the northward TWWC and weakens the southward ZMCC (Liu et al., 2007; Lee and Chao, 2003). The variation of the TWWC and ZMCC leads to trapping of the river-derived sediments in the YRE and formation of a mud area in this region, which is another reason why a deposition center forms near the YRE. But the deposition near the YRE is a short-term process which changes in the winter, as the ZMCC intensifies in the winter and carries the sediments deposited near the YRE southward along the inner shelf. Therefore, a large amount of fine sediments are re-suspended and transported southward and forms the ZMCMA, which will also transports a major portion of the associated PAHs into the ZMCMA. The results of our study showed that the PAHs concentration was relative high in the mud area of the YRE and IACZ, which is consistent with the distribution pattern of fine sediments controlled by the hydrodynamic conditions.

3.4. Deposition flux of PAHs

Deposition flux of PAHs was calcuated in this study using the Map Algebra technology with ArcGIS 10.2 (Fig. 7). The total deposition flux of PAHs calculated for approximately 50 000 km^2 in the YRE and IACZ was about 107.8 t a^{-1}. The annual flux of PAHs discharged into the YRE through Yangtze River was more than 369 t (Qi et al., 2014). Therefore, the deposition flux of PAHs in our study area accounted for about 29.2% of the total annual flux of the PAHs discharged into ECS. Deposition flux of the mud areas in the Yangtze estuarine-inner shelf (include the YREMA and ZMCMA; about 80,000 km^2) was estimated to be 152 t a^{-1} (Lin et al., 2013). Therefore, the deposition flux of PAHs in our study area accounted for about 70.9% of Lin et al. (2013) as our study area was smaller. Our study area is located at the YRE and the north part of ZMCMA (Fig. 1b,c) but Lin's study area occupied most of the mud area (Lin et al., 2013). Previous studies have demonstrated that about 32% of the sediment was transported from the Yangtze River and accumulated in the ZMCMA (DeMaster et al., 1985; Liu et al., 2007), implying that about 32% of the sedimentary PAHs are transported and accumulated in the ZMCMA. Thus, about 32% of the PAHs calculated by Lin et al. (2013), nearly 48.6 t of PAHs were deposited in the south part of the ZMCMA. So, the deposition flux in the YRE and the north part of ZMCMA was about 103.4 t, which is consistent with our result. A comparison with other continental shelves in the world is presented in Table S2. The deposition flux of PAHs in the study area is much higher than the Southern Bohai Sea, the Yellow Sea, and the Mediterranean Sea.

4. Conclusions

In the present study, sources and distribution patterns of 16 priority PAHs in surface sediments from the YRE and IACZ were investigated, and the influenced factors (i.e. granularity effect and hydrodynamics) were also discussed. The total concentration of PAHs ranged from 27.2 ng g^{-1} to 621.6 ng g^{-1} with an average value of 160.1 ng g^{-1}. Spatially, the distribution pattern of PAHs exhibited an increasing trend from north to south, and tended to decrease with increasing distance between the estuary and the IACZ. The result of PMF model showed that coal combustion, petrogenic source, wood combustion and traffic source are the four sources of PAHs in surface sediments from the YRE and IACZ. The distribution patterns of PAHs were consistent with sediment grain-size. In addition, marine dynamics in the study area are very complicated, which controlled the distribution patterns of sediments and associated PAHs. Overall, the distribution patterns of PAHs in the study area were influenced by several factors such as sediment grain-size and marine dynamics. The results of this study advance the understanding of the intensive economic activities to the coastal environments, and provide useful information to the PAHs management in the YRE and IACZ.

Acknowledgements

The study was supported by the National Basic Research Program of China (Grant No. 2013CB956503) and the Natural Science Foundation of China (Grant No. 41471431).

Appendix A. Supplementary data

Supplementary data related to this article can be found at http://dx.doi.org/10.1016/j.chemosphere.2016.07.075

References

Ali, U., Syed, J.H., Junwen, L., et al., 2014. Assessing the relationship and influence of black carbon on distribution status of organochlorines in the coastal sediments from Pakistan. Environ. Pollut. 190, 82–90.

Barakat, A.O., Mostafa, A.R., Wade, T.L., et al., 2011. Distribution and characteristics of PAHs in sediments from the Mediterranean coastal environment of Egypt. Mar. Pollut. Bull. 62 (9), 1969–1978.

Bianchi, T.S., Allison, M.A., 2009. Large-river delta-front estuaries as natural "recorders" of global environmental change. P. Natl. A. Sci. 106 (20), 8085–8092.

Bian, H.Y., Li, Z.Y., Liu, P., et al., 2010. Spatial distribution and deposition history of nonylphenol and bisphenol A in sediments from the Changjiang river (Yangtze

River) estuary and its adjacent East China Sea. Acta. Oceanol. Sin. 29 (5), 44–51.
Chen, S.J., Luo, X.J., Mai, B.X., 2006. Distribution and mass inventories of polycyclic aromatic hydrocarbons and organochlorine pesticides in sediments of the Pearl River Estuary and the Northern South China Sea. Environ. Sci. Technol. 40 (3), 709–714.
Comero, S., Vaccaro, S., Locoro, G., et al., 2014. Characterization of the Danube River sediments using the PMF multivariate approach. Chemosphere 95, 329–335.
DeMaster, D.J., McKee, B.A., Nittrouer, C.A., et al., 1985. Rates of sediment accumulation and particle reworking based on radiochemical measurements from continental shelf deposits in the East China Sea. Cont. Shelf. Res. 4 (1–2), 143–158.
Duan, L.Y., Wang, Z.H., Li, M.T., et al., 2005. ^{210}Pb distribution of the Changjiang estuarine sedmient and the implications to sedmientary environment. Acta Sedimentol. Sin. 23 (3), 514–522 (In Chinese with English abstract).
Fang, Y., Chen, Y.J., Tian, C.G., et al., 2015. Flux and budget of BC in the continental shelf seas adjacent to Chinese high BC emission source regions. Glob. Biogeochem. Cy 29, 957–972.
Gao, S., Cheng, P., Wang, Y.P., Cao, Q.Y., 2000. Characteristics of suspended sediment concentrations over the areas adjacent to the Changjiang River estuary, the summer of 1998. Mar. Sci. Bull. 2 (1), 14–24.
Gao, S., Wang, Y.P., 2008. Changes in material fluxes from the Changjiang River and their implications on the adjoining continental shelf ecosystem. Cont. Shelf. Res. 28 (12), 1490–1500.
Gao, S., Wang, Y.P., Gao, J.H., 2011. Sediment retention at the Changjiang subaqueous delta over a 57 year period, in response to catchment changes. Estuar. Coast. Shelf S 95 (1), 29–38.
Guo, Z.G., Lin, T., Zhang, G., et al., 2007. The sedimentary fluxes of polycyclic aromatic hydrocarbons in the Yangtze River Estuary coastal sea for the past century. Sci. Total Environ. 386 (1–3), 33–41.
He, H., Hu, G.J., Sun, C., et al., 2011. Trace analysis of persistent toxic substances in the main stream of Jiangsu section of the Yangtze River, China. Environ. Sci. Pollut. R. 18 (4), 638–648.
He, X.R., Pang, Y., Song, X.J., et al., 2014. Distribution, sources and ecological risk assessment of PAHs in surface sediments from Guan River Estuary, China. Mar. Pollut. Bull. 80 (1), 52–58.
Hopke, P.K., 2003. Recent developments in receptor modeling. J. Chemom. 17 (5), 255–265.
Hung, C.C., Gong, G.C., Ko, F.C., et al., 2011. Polycyclic aromatic hydrocarbons in surface sediments of the East China Sea and their relationship with carbonaceous materials. Mar. Pollut. Bull. 63, 464–470.
Huang, L., Zhang, G.S., 2015. Distribution of black carbon in the sediments from the Yangtze River and their correlations with polycyclic aromatic hydrocarbons. Earth Environ. 43 (2), 159–166 (In Chinese with English abstract).
Khalili, N.R., Scheff, P.A., Holsen, T.M., 1995. PAH source fingerprints for coke ovens, diesel and, gasoline engines, highway tunnels, and wood combustion emissions. Atmos. Environ. 29 (4), 533–542.
Kim, G.B., Maruya, K.A., Lee, R.F., et al., 1999. Distribution and sources of polycyclic aromatic hydrocarbons in sediments from Kyeonggi Bay, Korea. Mar. Pollut. Bull. 38, 7–15.
Lee, H.J., Chao, S.Y., 2003. A climatological description of circulation in and around the East China Sea. Deep-Sea. Res. PT II. 50 (6), 1065–1084.
Li, A., Jang, J.K., Scheff, P.A., et al., 2003. Application of EPA CMB8.2 model for source apportionment of sediment PAHs in lake Calumet, Chicago. Environ. Sci. Technol. 37, 2958–2965.
Li, B., Feng, C., Li, X., et al., 2012. Spatial distribution and source apportionment of PAHs in surficial sediments of the Yangtze Estuary, China. Mar. Pollut. Bull. 64 (3), 636–643.
Li, G., Xia, X., Yang, Z., et al., 2006. Distribution and sources of polycyclic aromatic hydrocarbons in the middle and lower reaches of the Yellow River, China. Environ. Pollut. 144 (3), 985–993.
Li, J., Dong, H., Zhang, D., et al., 2015. Sources and ecological risk assessment of PAHs in surface sediments from Bohai Sea and northern part of the Yellow Sea, China. Mar. Pollut. Bull. 96 (1), 485–490.
Lima, A.L., Farrington, J.W., Reddy, C.M., 2005. Combustion-derived polycyclic aromatic hydrocarbons in the environment—a review. Environ. Forensics 6, 109–131.
Lin, S., Hsieh, I.J., Huang, K.M., et al., 2002. Influence of the Yangtze River and grain size on the spatial variations of heavy metals and organic carbon in the East China Sea continental shelf sediments. Chem. Geol. 182 (2), 377–394.
Lin, T., Hu, L.M., Guo, Z.G., et al., 2013. Deposition fluxes and fate of polycyclic aromatic hydrocarbons in theYangtze River estuarine-inner shelf in the EastChina Sea. Glob. Biogeochem. Cy 27, 77–87.
Liu, J.P., Xu, K.H., Li, A.C., et al., 2007. Flux and fate of Yangtze River sediment delivered to the East China Sea. Geomorphology 85 (3–4), 208–224.
Liu, J.P., Li, A.C., Xu, K.H., 2006. Sedimentary features of the Yangtze River-derived along-shelf clinoform deposit in the East China Sea. Cont. Shelf. Res. 26 (17), 2141–2156.
Liu, J.Y., Wang, J.Z., Guan, Y.F., et al., 2012. Use of aliphatic hydrocarbons to infer terrestrial organic matter in coastal marine sediments off China. Mar. Pollut. Bull. 64, 1940–1946.
Liu, Y., Gao, S., Wang, Y.P., et al., 2014. Distal mud deposits associated with the Pearl River over the northwestern continental shelf of the South China Sea. Mar. Geol. 347 (1), 43–57.
Liu, Y., Chen, L., Huang, Q., et al., 2009. Source apportionment of polycyclic aromatic hydrocarbons (PAHs) in surface sediments of the Huangpu River, Shanghai, China. Sci. Total Environ. 407, 2931–2938.
Mcmanus, J., 1988. Grain size determination and interpretation. In: Tucker, M. (Ed.), Techniques in Sedimentology. Black-well, Oxford, pp. 63–85.
Milliman, J.D., Hsueh, Y., Hu, D.X., et al., 1984. Tidal phase control of sediment discharge from the Yangtze River. Estuar. Coast. Shelf. S. 19, 119–128.
Milliman, J.D., Syvitski, J.P.M., 1992. Geomorphic/tectonic control of sediment discharge to the ocean: the importance of small mountainous rivers. J. Geol. 100, 525–544.
NBSC (National Bureau of Statistics of China), 2014. China Economic Yearbook in 2014 (Beijing).
Paatero, P., Tapper, U., 1994. Positive matrix factorization: a non-negative factor model with optimal utilization of error estimates of data values. Environmetrics 5 (2), 111–126.
Qi, W., Müller, B., Pernet-Coudrier, B., et al., 2014. Organic micropollutants in the Yangtze River: seasonal occurrence and annual loads. Sci. Total Environ. 472, 789–799.
Qiao, M., Wang, C., Huang, S., et al., 2006. Composition, sources, and potential toxicological significance of PAHs in the surface sediments of the Meiliang Bay, Taihu Lake, China. Environ. Int. 32, 28–33.
Qin, Y.W., Zheng, B.H., Lei, K., et al., 2011. Distribution and mass inventory of polycyclic aromatic hydrocarbons in the sediments of the south Bohai Sea, China. Mar. Pollut. Bull. 62, 371–376.
Qin, Y.S., Zhao, Y.Y., Chen, L.R., et al., 1987. Geology of the East China Sea. China Science Press, Beijing, pp. 290.
Shi, G.L., Xu, J., Peng, X., 2016. Using a new WALSPMF model to quantify the source contributions to PM2. 5 at a harbour site in China. Atmos. Environ. 126, 66–75.
Shi, G.L., Li, X., Feng, Y.C., 2009. Combined source apportionment, using positive matrix factorization–chemical mass balance and principal component analysis/multiple linear regression–chemical mass balance models. Atmos. Environ. 43 (18), 2929–2937.
Simoneit, B.R.T., 2002. Biomass burning – a review of organic tracers for smoke from incomplete combustion. Appl. Geochem 17, 129–162.
Simcik, M.F., Eisenreich, S.J., Lioy, P.J., 1999. Source apportionment and source/sink relationships of PAHs in the coastal atmosphere of Chicago and Lake Michigan. Atmos. Environ. 33, 5071–5079.
Sofowote, U.M., McCarry, B.E., Marvin, C.H., 2008. Source apportionment of PAH in Hamilton Harbour suspended sediments: comparison of two factor analysis methods. Environ. Sci. Technol. 42 (16), 6007–6014.
Su, J.L., Wang, K.S., 1986. The suspended sediment balance in Changjiang estuary. Estuar. Coast. Shelf. S. 23, 81–98.
Su, C.C., Huh, C.A., 2002. ^{210}Pb, ^{137}Cs and ^{239,240}Pu in East China Sea sediments: sources, pathways and budgets of sediments and radionuclides. Mar. Geol. 183 (1), 163–178.
Sverdrup, L.E., Nielsen, T., Krogh, P.H., 2002. Soil ecotoxicity of polycyclic aromatic hydrocarbons in relation to soil sorption, lipophilicity, and water solubility. Environ. Sci. Technol. 36, 2429–2435.
Tian, Y.Z., Shi, G.L., Han, B., 2015. Using an improved Source Directional Apportionment method to quantify the PM 2.5 source contributions from various directions in a megacity in China. Chemosphere 119, 750–756.
Traffic Management Bureau of The Public Security Ministry, 2015. http://www.mps.gov.cn/n2255040/n4908728/c4929117/content.html.
US EPA, 2014. EPA Positive Matrix Factorization (PMF) 5.0 Fundamentals & User Guide. Online available at: http://www.epa.gov/heasd/research/pmf.html.
Wang, C.H., Wu, S.H., Zhou, S.L., et al., 2015. Polycyclic aromatic hydrocarbons in soils from urban to rural areas in Nanjing: concentration, source, spatial distribution, and potential human health risk. Sci. Total Environ. 527–528, 375–383.
Wang, D., Tian, F., Yang, M., et al., 2009. Application of positive matrix factorization to identify potential sources of PAHs in soil of Dalian, China. Environ. Pollut. 157, 1559–1564.
Wang, J.Z., Guan, Y.F., Ni, H.G., et al., 2007. Polycyclic aromatic hydrocarbons in riverine runoff of the Pearl River Delta (China): concentrations, fluxes, and fate. Environ. Sci. Technol. 41 (16), 5614–5619.
Wang, X., Shi, X.F., Wang, G.Q., et al., 2013. Sedimentation Rates and its indication to distribution to distribution of Yangtze sediment supply around the Yangtze (Changjiang) River Estuary and its adjacent area, China. Earth S. J. China Univ. Geosci. 38 (4), 763–775 (In Chinese with English abstract).
Wang, Y.H., 2003. Reformation Mechanism and Features of Dynamic Sediment in Flood Channels of the Changjiang Estuary (Doctoral dissertation) (In Chinese with English abstract).
Yang, Z., Wang, H., Saito, Y., et al., 2006. Dam impacts on the Changjiang (Yangtze) river sediment discharge to the sea: the past 55 years and after the Three Gorges Dam. Water Resour. Res. 42, W04407.
Yim, U.H., Hong, S.H., Ha, S.Y., 2014. Source-and region-specific distribution of polycyclic aromatic hydrocarbons in sediments from Jinhae Bay, Korea. Sci. Total Environ. 470, 1485–1493.
Yunker, M.B., Macdonald, R.W., Vingarzan, R., et al., 2002. PAHs in the Fraser River basin: a critical appraisal of PAH ratios as indicators of PAH source and composition. Org. Geochem 33, 489–515.
Yu, W., Liu, R., Wang, J., et al., 2015. Source apportionment of PAHs in surface sediments using positive matrix factorization combined with GIS for the estuarine area of the Yangtze River, China. Chemosphere 134, 263–271.
Zhang, R., Pan, S.M., Wang, Y.P., et al., 2009. Sedimentation rates and characteristics of radionuclide ^{210}Pb at the subaqueous delta in Changjiang Estuary. Acta Sedimentol. Sin. 27 (4), 703–713 (In Chinese with English abstract).

Zhang, Y., Guo, C.S., Xu, J., et al., 2012. Potential source contributions and risk assessment of PAHs in sediments from Taihu Lake, China: comparison of three receptor models. Water Res. 46, 3065–3073.
Zhang, Y.X., Tao, S., 2009. Global atmospheric emission inventory of polycyclic aromatic hydrocarbons (PAHs) for 2004. Atmos. Environ. 43, 812–819.
Zhou, S., Yang, H., Zhang, A., et al., 2014. Distribution of organochlorine pesticides in sediments from Yangtze River Estuary and the adjacent East China Sea, Implication of transport, sources and trends. Chemosphere 114, 26–34.
Zeng, L., Zhao, Z., Li, H., et al., 2012. Distribution of short chain chlorinated paraffins in marine sediments of the East China Sea: influencing factors, transport and implications. Environ. Sci. Technol. 46 (18), 9898–9906.